

## Research Article

# Evolution of Mesopores in Monolithic Macroporous Ethylene-Bridged Polysilsesquioxane Gels Incorporated with Nonionic Surfactant

Atsushi Mushiake, Kazuyoshi Kanamori, and Kazuki Nakanishi

Department of Chemistry, Graduate School of Science, Kyoto University, Kitashirakawa, Sakyo-ku, Kyoto 606-8502, Japan

Correspondence should be addressed to Kazuki Nakanishi, kazuki@kuchem.kyoto-u.ac.jp

Received 11 July 2012; Accepted 4 September 2012

Academic Editor: Takahiro Gunji

Copyright © 2012 Atsushi Mushiake et al. This is an open access article distributed under the Creative Commons Attribution License, which permits unrestricted use, distribution, and reproduction in any medium, provided the original work is properly cited.

By combining the micellar templating in nanometer scale with the polymerization-induced phase separation in micrometer scale, ethylene-bridged polysilsesquioxane gels with hierarchical macropores and mesopores are prepared. The difference of mesopore structures depending on the method of the solvent removal has been observed by the X-ray diffraction and the nitrogen adsorption-desorption measurements. During the hydrothermal treatment under the basic condition, the reorganization of the polysilsesquioxane gel network occurred differently depending on the alkoxy group contained in the precursors. From  $^{29}\text{Si}$  CP/MAS NMR measurements, it was revealed that the crosslinking density of the hydrothermally treated gels was increased so that the highly ordered mesostructure of the wet gel could be preserved even after the evaporative drying of solvent.

## 1. Introduction

Synthesis of solids with surfactant-templated mesopores is an established procedure where various precursors can be used to produce metal oxides and metallocxane-based organic-inorganic hybrid materials [1–3]. It has been reported that monolithic ethane-silica gels with well-defined cocontinuous macropores and highly ordered mesopores has been synthesized via spontaneous route from the ethylene bridged silicon alkoxide with the aid of a structure-directing agent [4, 5]. These materials have higher alkaline resistance than pure silica gels due to their Si-C bond, so they can favorably be applied to catalyst supports, adsorbents, and separation media. The synthesis process is based upon alkoxy-derived sol-gel reactions in the presence of water-soluble organic polymers, such as poly(ethylene oxide). During the polymerization reaction of silicon alkoxides in an acidic condition, spinodal decomposition-type phase separation occurs concurrently with gelation, resulting in the formation of bicontinuous gel-rich and solvent-rich phases on the length scale of micrometers. In the pure silica system, subsequent solvent exchange with a basic aqueous solution

and aging treatment generates the mesopores in the gel-rich phase via a process of dissolution/reprecipitation (Ostwald ripening) [6]. Upon evaporation drying, the gel-rich phase becomes mesoporous gel skeletons, and the solvent-rich phase turns into macropores that serve as flow-through pores. The macropores allow facile transport of fluid, while the mesopores offer extended surface area that facilitates the contacts between fluid and the solid surface [7].

In contrast to the pure silica system, the dissolution/reprecipitation hardly occurs in the bridged polysilsesquioxane system due to higher resistance of siloxane bonds against nucleophilic attacks. It is thus difficult to form mesopores in the gel skeletons just by solvent exchange with a basic solution. It is reported, however, that the relatively strong hydrothermal treatment of macroporous wet titania ( $\text{TiO}_2$ ) gels which have negligible solubility in water results in the development of mesoporous structure [8]. It is therefore expected that mesopores in bridged polysilsesquioxane gels are also developed by appropriate hydrothermal treatments even if the structural evolution does not occur by dissolution/reprecipitation process. Although there are some reports on the formation of micropores in bridged

polysilsesquioxanes [9–11], almost nothing is known on the development of mesopores. In this paper, we investigate the effect on the mesostructure of the mode of solvent removal and conditions of hydrothermal treatments under weakly basic conditions. We also compare the difference between ethylene-bridged precursors: one with methoxy and the other ethoxy groups as hydrolysable ligands.

## 2. Experimental

**2.1. Chemicals.** The 1,2-bis(trimethoxysilyl)ethane, BTME, and 1,2-bis(triethoxysilyl)ethane, BTEE, purchased from Sigma-Aldrich, were used as precursors for silsesquioxane network. As structure-directing agents, poly(ethylene glycol)<sub>20</sub>-block-poly(propylene glycol)<sub>70</sub>-block-poly(ethylene glycol)<sub>20</sub>, with average molecular mass of 5800, and poly(ethylene glycol)<sub>106</sub>-block-poly(propylene glycol)<sub>70</sub>-block-poly(ethylene glycol)<sub>106</sub>, with average molecular mass of 12600, obtained from Sigma-Aldrich (equivalent to Pluronic P123 and F127, BASF) were used. Acetic acid (HOAc, 99.7 wt%), a product of Kishida Chemical Co., Ltd., and nitric acid (HNO<sub>3</sub>, 60 wt%), a product of Hayashi Pure Chemical Industry Co., Ltd., were used as acid catalysts. Urea, a product of Hayashi Pure Chemical Industry Co., Ltd., was adopted for the purpose of raising solution pH homogeneously within a wet gel by the gradual generation of ammonia due to its hydrolysis. All reagents were used as received.

**2.2. Synthesis Procedure.** In the BTME-HOAc-P123-Urea system, BTME (2.14 g) was added to the homogeneous solution of P123 (2.2 g), urea (1.0 g), and 0.01 M acetic acid (15 g) under vigorous stirring at 0°C for hydrolysis. After 10 min of stirring, the resultant solution was kept at 60°C for gelation/aging. After 48 h, the solvent was removed by evaporative drying method or supercritical drying method. Hereinafter, we denote the samples prepared by these methods as ME-EvD and ME-SCD, respectively. Also, the hydrothermal treatment was conducted at 150°C using aged gels for 20 h in an autoclave under a weakly basic condition. Then, the wet gel was evaporatively dried. Obtained sample is denoted as ME-HyT.

In the BTEE-HNO<sub>3</sub>-P123 system, BTEE (1.92 g) was added to the homogeneous solution of P123 (1.6 g) and 0.1 M nitric acid (16 g) under vigorous stirring at 0°C for hydrolysis. Due to considerably low reactivity of ethoxy ligands towards hydrolysis, the use of nitric acid was mandatory. After 20 min of stirring, the resultant solution was kept at 60°C for 24 h. After gelation/aging, the solvent was removed by evaporative drying method or supercritical drying method, and we denote the samples prepared in these method as EE-EvD and EE-SCD, respectively. The hydrothermal treatment was conducted at 150°C using aged gels for 20 h in an autoclave after the solvent exchange with 1.0 M aqueous solution of urea. The exchange of solvent with 1.0 M urea solution is necessary to ensure the weakly basic condition during the hydrothermal treatment. Samples obtained by the evaporative drying of the hydrothermally

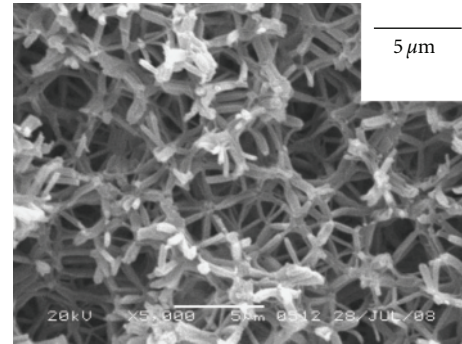


FIGURE 1: SEM image of the ME-EvD sample.

treated gels are denoted as EE-HyT. Some of dried gels were heat-treated at 250°C for 2 h to remove organic components. The heat-treatment condition was selected so as not to decompose the bridging hydrocarbon chain while removing other organic constituents as completely as possible.

**2.3. Characterization.** The morphology of dried gels was observed by a scanning electron microscope (SEM, JSM-6060S, JEOL Ltd., Japan). X-ray diffraction (XRD) analysis with Ni-filtered Cu K $\alpha$  radiation (RINT Ultima III, Rigaku Co., Japan) for heat-treated gels was performed at room temperature. Nitrogen sorption measurements for heat-treated gels were performed to obtain mesopore size distribution with BELSORP-mini II (BEL JAPAN, Japan). Samples were outgassed under vacuum at 80°C for 24 h prior to measurements. The adsorption branch was used for the calculation of pore size distribution by BJH method. An NMR spectrometer Chemagnetics CMX-400 has been operated for dried gels under a static magnetic field of 9.4 T. The contact time for the cross polarization was fixed at 5.0 ms and the rate of sample spinning was set to 6 kHz. The <sup>29</sup>Si chemical shifts were expressed as values relative to tetramethylsilane (Me<sub>4</sub>Si) by using the resonance line at -34 ppm for PDMS crystals as an external reference.

## 3. Results and Discussion

### 3.1. BTME-HOAc-P123-Urea System

**3.1.1. Macromorphology.** Figure 1 shows the typical SEM image of the ME-EvD sample. Thin columnar gel skeletons are fully connected at nodes comprising co-continuous and high-porosity structure. The macropore size is a few micrometers and the macroporosity reaches ca. 90%. The columnar skeletons contain cylindrical mesopores which are 2D hexagonally ordered along with the long axes as shown below in detail.

**3.1.2. X-Ray Diffraction.** Figure 2 shows XRD patterns of the ME-EvD, the ME-SCD, and the ME-HyT samples. The ME-EvD sample shows only single broad peak at higher scattering angle than the other two samples. On the other hand, in addition to the sharp (10) peak, the (11) and

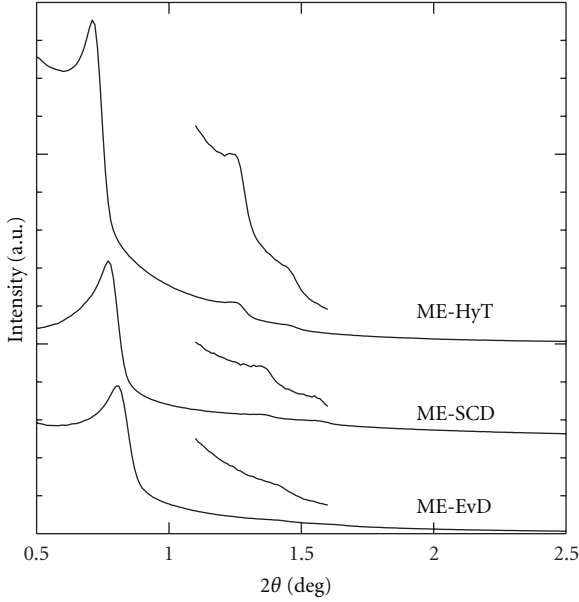


FIGURE 2: XRD patterns of the ME-EvD, the ME-SCD, and the ME-HyT samples.

(20) peaks are observed for the ME-SCD and the ME-HyT gels. This indicates that the periodicity of 2D hexagonal symmetry in an extended length scale is preserved after the solvent removal. In the process of evaporative drying, the large shrinkage occurs on the ME-EvD sample, and ordered mesostructure of the wet gels is collapsed. The robust ME-HyT sample maintains the mesostructure of the wet gel due to the highly cross-linked structure during the hydrothermal treatment. The ME-SCD sample also shows higher-order peaks with weaker intensity than those of ME-HyT. This result is expected because the capillary force should not work on the gel networks during the supercritical drying process. In addition, the intensity of the ME-HyT sample increases around  $2\theta = 0.5^\circ$ . This suggests that additional heterogeneity, pores for example, on a longer length scale than that of template pores is present in the ME-HyT sample.

**3.1.3. Nitrogen Sorption Measurements.** The nitrogen adsorption-desorption isotherms and differential pore size distributions calculated by BJH method of respective gel samples are shown in Figure 3. The isotherms for three samples are classified to type IV with type H1 hysteresis of IUPAC classification, which show the presence of cylindrical mesopores. The mesopore size and the pore volume of ME-EvD sample are smaller than the others due to the larger drying shrinkage. The pore volume of ME-SCD sample is larger than that of ME-EvD sample due to the limited shrinkage. In addition, the mesopore size of ME-HyT is much larger than those of others. This is presumably because some of the adjacent mesopores were merged to form larger mesopores during the hydrothermal treatment. Unlike the pure silica system, a process of dissolution/reprecipitation (Ostwald ripening) hardly occurs in bridged polysilsesquioxane gels under the basic condition. This is

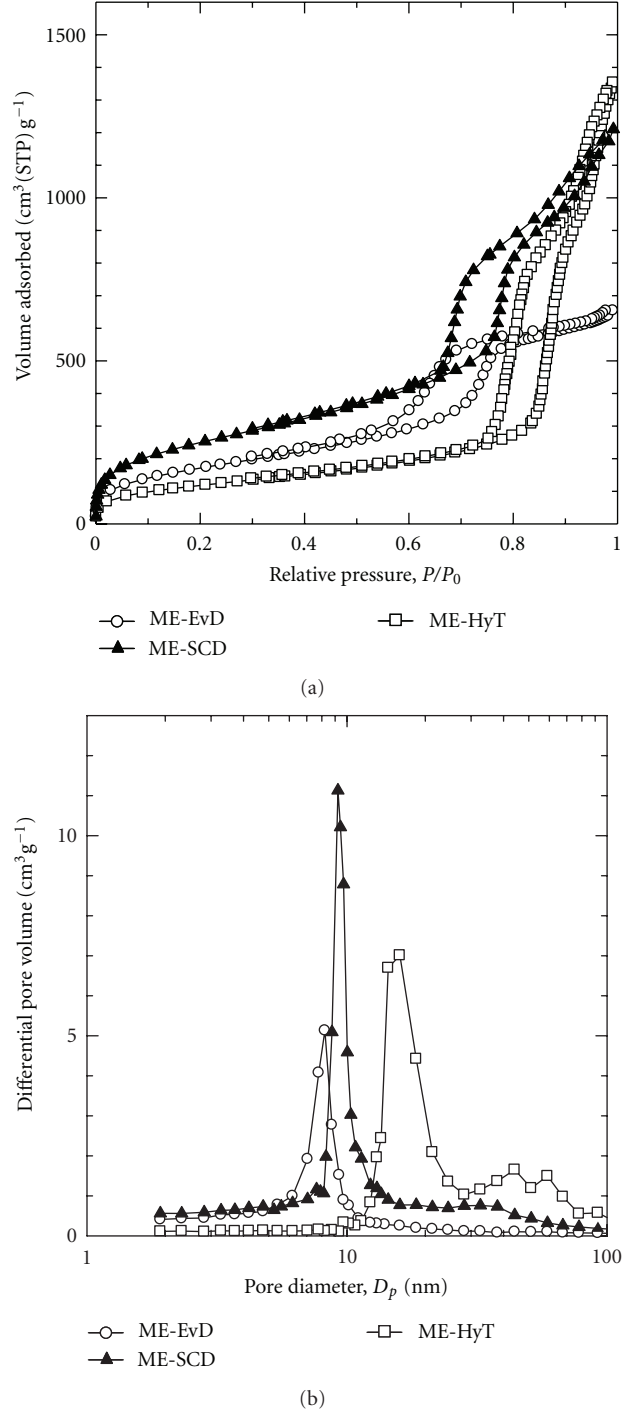


FIGURE 3: Adsorption-desorption isotherms (a) and differential pore size distributions (b) of the ME-EvD, the ME-SCD, and the ME-HyT samples.

mainly due to the limited solubility of polysilsesquioxane network owing to the Si–ethylene bond that suppresses the cleavage of Si–O bonds by nucleophilic attacks [12]. The drastic reorganization of siloxane network should necessarily be accompanied by significant change in connectivity of Si–O network.

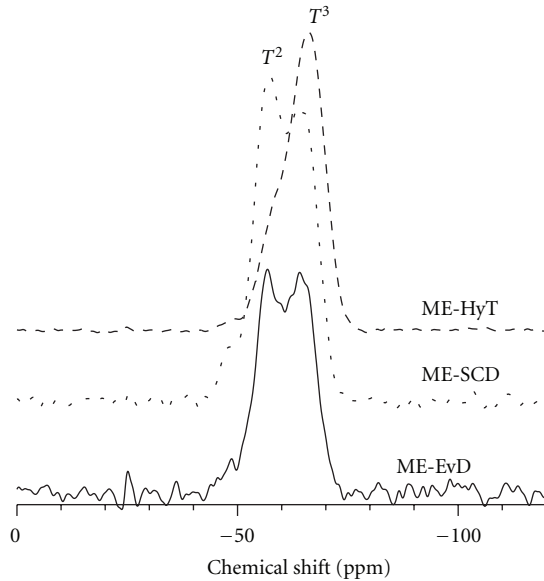


FIGURE 4:  $^{29}\text{Si}$  CP/MAS NMR spectra of the ME-EvD, the ME-SCD, and the ME-HyT samples.

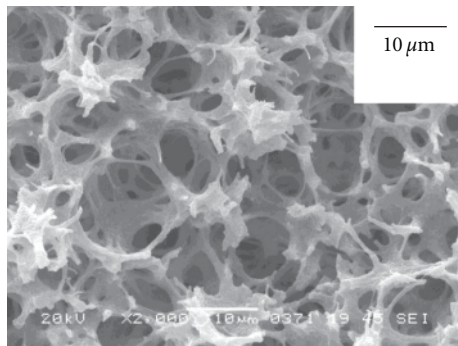


FIGURE 5: SEM image of the EE-EvD sample.

**3.1.4.  $^{29}\text{Si}$  CP/MAS NMR Measurements.** The  $^{29}\text{Si}$  CP/MAS NMR spectra of respective gel samples are shown in Figure 4. The peaks at  $-48$ ,  $-57$ , and  $-64$  ppm are assigned to  $T^1$ ,  $T^2$ , and  $T^3$  Si, respectively.  $T^n$  indicates the Si in the formula of  $\text{R}'\text{Si}(\text{OSi})_n(\text{OR})_{3-n}$  where  $\text{R}'$  is ethylene bridge and R is methyl group or proton. In the ME-EvD and the ME-SCD samples, the  $T^2$  peak is the largest. On the other hand, the NMR spectrum drastically changes in the ME-HyT sample:  $T^3$  becomes the largest, and  $T^2$  decreases instead. This indicates that the hydrothermal treatment induces reorganization of gel network in such a way that crosslink density is increased. The change confirmed by  $^{29}\text{Si}$  CP/MAS NMR is in good agreement with the development of coarser mesopores and increased porosity where rigid frameworks are developed by consuming finer structures.

### 3.2. BTEE- $\text{HNO}_3$ -P123 System

**3.2.1. Macro-Morphology.** Figure 5 shows the SEM image of the EE-EvD sample. The structure is coarser co-continuous than the ME-EvD sample. The average macropore size of

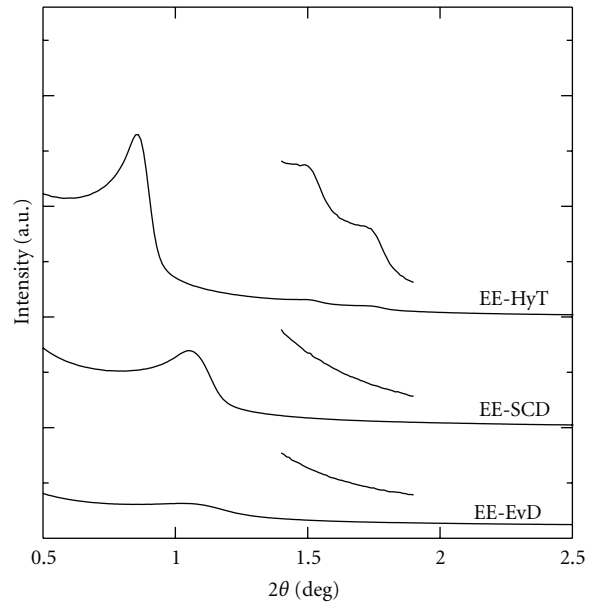


FIGURE 6: XRD patterns of the EE-EvD, the EE-SCD, and the EE-HyT samples.

the EE-EvD sample is  $3\ \mu\text{m}$  in contrast to  $1\ \mu\text{m}$  of the ME-EvD sample, and columnar skeletons are not observed. This suggests mesopores of the EE-EvD sample are not as highly ordered as those of the ME-EvD sample. The main reason is ethanol generated by the hydrolysis of BTEE that hinders the micelle formation more strongly than the case of methanol generated after hydrolysis of BTME.

**3.2.2. X-Ray Diffraction.** Figure 6 shows XRD patterns of the EE-EvD, the EE-SCD, and the EE-HyT samples. Not only the EE-EvD sample, but also the EE-SCD sample shows only single broad peak at higher scattering angle compared with the ME-EvD and the ME-SCD samples. The EE-HyT sample, however, shows highly ordered peak of 2D hexagonal symmetry due to the robust macroframework. In the EE-SCD sample, highly ordered mesostructure of the wet gel is collapsed and shrinkage occurs due to the high pressure during supercritical drying. On the other hand, the highly ordered mesostructure of the ME-SCD sample is preserved after supercritical drying. It can be reasonably assumed that the crosslink density of the gels prepared in the BTEE- $\text{HNO}_3$ -P123 system is lower and the gels are more fragile than the gels prepared in the BTME-HOAc-P123-Urea system. In the BTME-HOAc-Urea system, the hydrolysis is conducted in a weakly acidic condition, and the following gelation process occurs in neutral or weakly basic condition. Hydrolysis of starting alkoxides are complete and high probability of crosslinking is available in the polycondensation stage. The BTEE- $\text{HNO}_3$  system, on the other hand, is crosslinked in an acidic condition where less branching and crosslinking density is expected.

**3.2.3. Nitrogen Sorption Measurements.** The nitrogen adsorption-desorption isotherms and differential pore

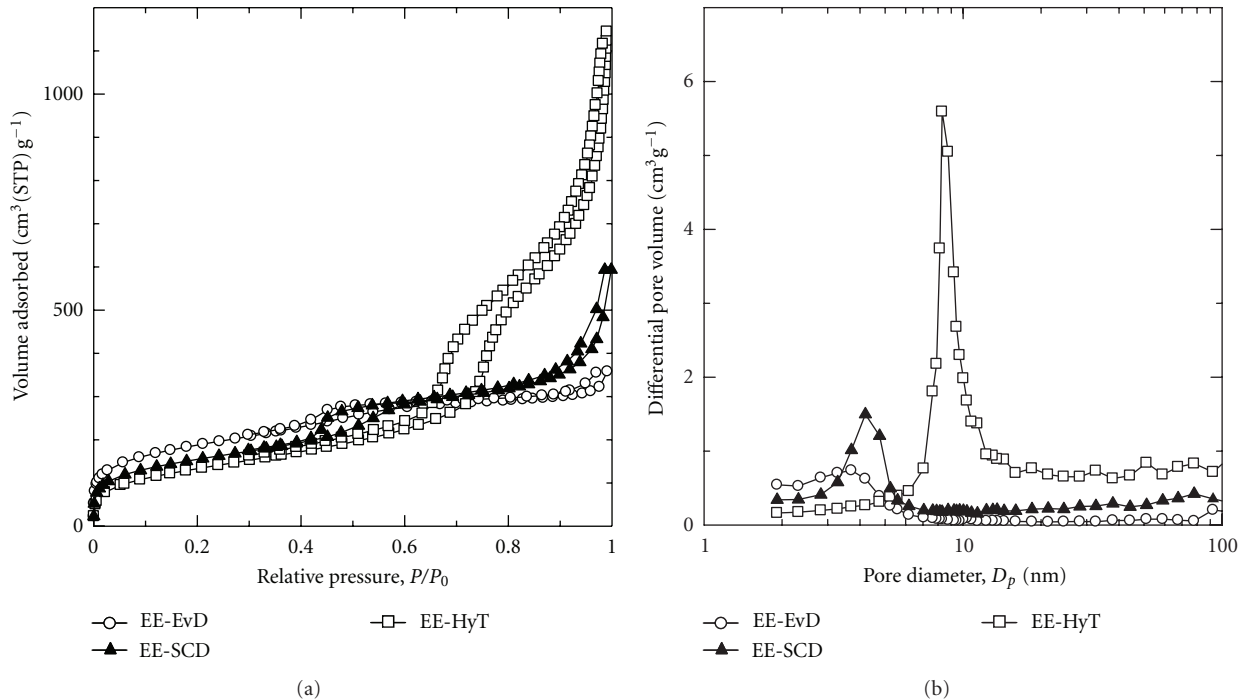


FIGURE 7: Adsorption-desorption isotherms (a) and differential pore size distributions (b) of the EE-EvD, the EE-SCD and the EE-HyT samples.

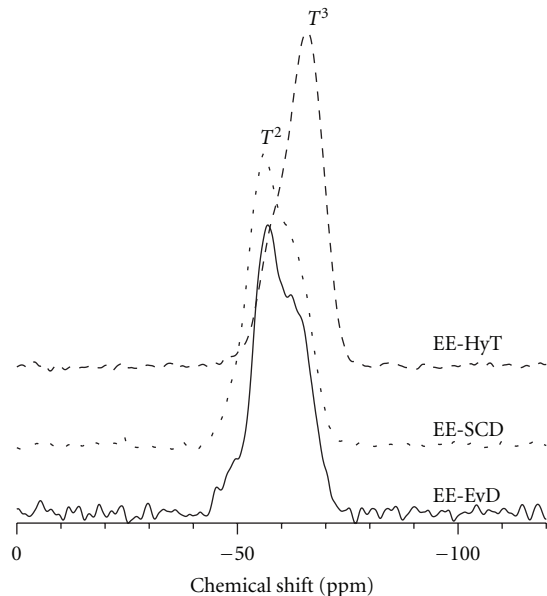


FIGURE 8:  $^{29}\text{Si}$  CP/MAS NMR spectra of the EE-EvD, the EE-SCD and the EE-HyT samples.

size distributions calculated by BJH method of respective samples are shown in Figure 7. Only the isotherm for the EE-HyT sample shows H1 hysteresis and the pore volume is much higher than those of the other two samples. By contrast, the pore volume and the mesopore size of the EE-SCD sample are very small due to the shrinkage during

supercritical drying even though those of the ME-SCD sample are large. This coincides with the fact of disordered pore structure evidence by the XRD measurement. The difference also suggests that gel networks prepared in the BTME-HNO<sub>3</sub>-P123 system are more fragile than the gels prepared in the BTME-HOAc-P123-Urea system.

**3.2.4.  $^{29}\text{Si}$  CP/MAS NMR Measurements.** The  $^{29}\text{Si}$  CP/MAS NMR spectra of respective samples are shown in Figure 8.  $T^n$  indicates the Si in the formula of  $\text{R}'\text{Si}(\text{OSi})_n(\text{OR})_{3-n}$  where  $\text{R}'$  is ethylene bridge and R is ethyl group or proton. In the EE-EvD and the EE-SCD samples, the  $T^2$  peak is the largest, and small  $T^1$  and  $T^3$  are observed. As with the BTME-HOAc-P123-Urea system,  $T^3$  becomes the largest, and  $T^2$  decrease their intensity in the EE-HyT sample. This again indicates the reorganization of gel network in BTME-HNO<sub>3</sub>-P123 system occurs and crosslinking is enhanced during the hydrothermal treatment. As a result, EE-HyT sample maintains their mesostructure of wet gel after evaporative drying. The peak ratio,  $T^2/T^3$  in the EE-EvD and the EE-SCD samples is much higher than that in the ME-EvD and the ME-SCD samples reflecting that the overall flexibility of the network is higher in BTME systems. Consequently, the EE-EvD sample shows broader single peak than the ME-EvD sample in the XRD measurements due to larger shrinkage during the evaporative drying process. The collapse of highly ordered mesostructure of the EE-SCD sample during the supercritical drying process can also be explained by the difference in crosslinking density.

## 4. Conclusions

Mesopore structure of ethylene-bridged polysilsesquioxane changed depending on the precursor and method of the solvent removal. By the hydrothermal treatment, reorganization of gel network occurred and crosslink density was increased. As a result, the highly ordered mesostructure was maintained after evaporative drying. The crosslink density of the gels prepared in the BTee-HNO<sub>3</sub>-P123 system was lower and the gels were more fragile than the gels prepared in BTMe-HOAc-P123-Urea system, and highly ordered mesostructure of the wet gels was collapsed during drying process without hydrothermal treatment. Gelation in higher pH conditions coupled with appropriate hydrothermal conditions are necessary to prepare well-defined hierarchically porous ethylene-bridged polysilsesquioxane monoliths.

## Acknowledgment

This work was partly supported by JST, ALCA Project.

## References

- [1] Yanagisawa, T. Shimizu, T. Kuroda, and K. Kato C, “The preparation of alkyltriaethylaminium-kaneinite complexes and their conversion to microporous materials,” *Bulletin of the Chemical Society of Japan*, vol. 63, no. 4, pp. 988–992, 1990.
- [2] C. T. Kresge, M. E. Leonowicz, W. J. Roth, J. C. Vartuli, and J. S. Beck, “Ordered mesoporous molecular sieves synthesized by a liquid-crystal template mechanism,” *Nature*, vol. 359, no. 6397, pp. 710–712, 1992.
- [3] S. Inagaki, Y. Fukushima, and K. Kuroda, “Synthesis of highly ordered mesoporous materials from a layered polysilicate,” *Journal of the Chemical Society, Chemical Communications*, no. 8, pp. 680–682, 1993.
- [4] K. Nakanishi, Y. Kobayashi, T. Amatani, K. Hirao, and T. Kodaira, “Spontaneous formation of hierarchical macro-mesoporous ethane-silica monolith,” *Chemistry of Materials*, vol. 16, no. 19, pp. 3652–3658, 2004.
- [5] K. Nakanishi, T. Amatani, S. Yano, and T. Kodaira, “Multiscale templating of siloxane gels via polymerization-induced phase separation,” *Chemistry of Materials*, vol. 20, no. 3, pp. 1108–1115, 2008.
- [6] R. Takahashi, K. Nakanishi, and N. Soga, “Insight on structural change in sol-gel-derived silica gel with aging under basic conditions for mesopore control,” *Journal of Sol-Gel Science and Technology*, vol. 33, no. 2, pp. 159–167, 2005.
- [7] K. Nakanishi and N. Tanaka, “Sol-gel with phase separation. Hierarchically porous materials optimized for high-performance liquid chromatography separations,” *Accounts of Chemical Research*, vol. 40, no. 9, pp. 863–873, 2007.
- [8] J. Konishi, K. Fujita, K. Nakanishi et al., “Sol-gel synthesis of macro-mesoporous titania monoliths and their applications to chromatographic separation media for organophosphate compounds,” *Journal of Chromatography A*, vol. 1216, no. 44, pp. 7375–7383, 2009.
- [9] H. W. Oviatt Jr., K. J. Shea, and J. H. Small, “Alkylene-bridged silsesquioxane sol-gel synthesis and xerogel characterization. Molecular requirements for porosity,” *Chemistry of Materials*, vol. 5, no. 7, pp. 943–950, 1993.
- [10] D. A. Loy, J. P. Carpenter, T. M. Alam et al., “Cyclization phenomena in the sol-gel polymerization of  $\alpha,\omega$ - bis(triethoxysilyl)alkanes and incorporation of the cyclic structures into network silsesquioxane polymers,” *Journal of the American Chemical Society*, vol. 121, no. 23, pp. 5413–5425, 1999.
- [11] B. Boury and R. J. P. Corriu, “Adjusting the porosity of a silica-based hybrid material,” *Advanced Materials*, vol. 12, no. 13, pp. 989–992, 2000.
- [12] K. D. Wyndham, J. E. O’Gara, T. H. Walter et al., “Characterization and evaluation of C<sub>18</sub> HPLC stationary phases based on ethyl-bridged hybrid organic/inorganic particles,” *Analytical Chemistry*, vol. 75, no. 24, pp. 6781–6788, 2003.



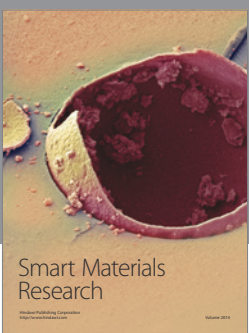
Journal of  
Nanotechnology



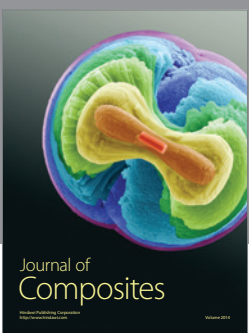
International Journal of  
Corrosion



International Journal of  
Polymer Science



Smart Materials  
Research



Journal of  
Composites



BioMed  
Research International

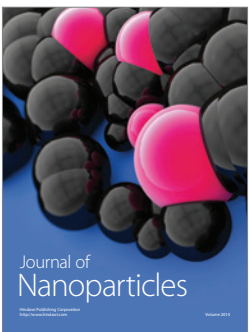


Hindawi

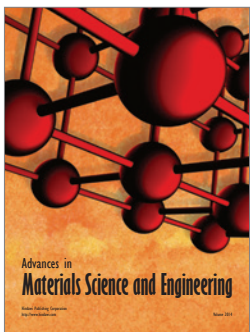
Submit your manuscripts at  
<http://www.hindawi.com>



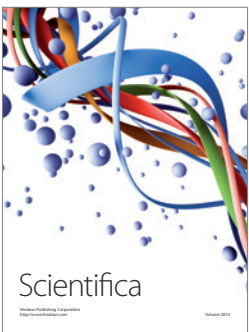
Journal of  
Materials



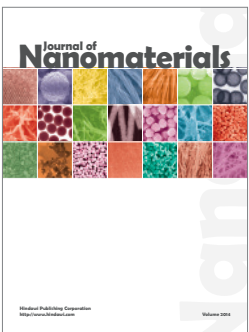
Journal of  
Nanoparticles



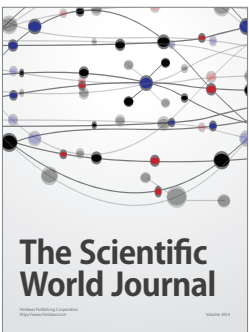
Advances in  
Materials Science and Engineering



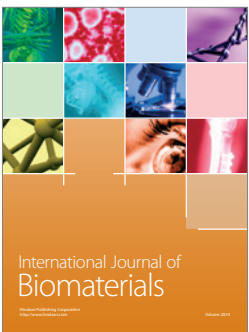
Scientifica



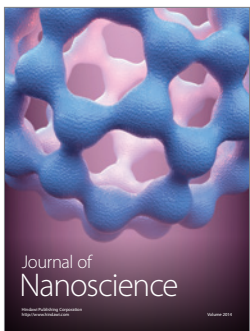
Journal of  
Nanomaterials



The Scientific  
World Journal



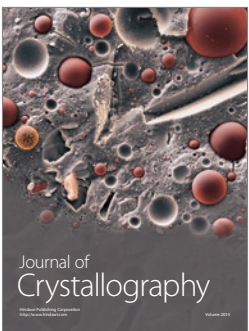
International Journal of  
Biomaterials



Journal of  
Nanoscience



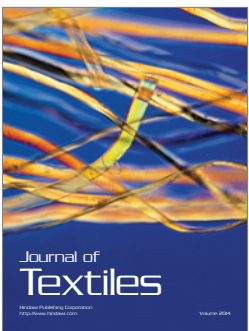
Journal of  
Coatings



Journal of  
Crystallography



Journal of  
Ceramics



Journal of  
Textiles